crystals

MDPI

Communication

Effect of Overheating Temperature on Thermal Cycling Creep Properties of K465 Superalloy

Xiaotong Guo [1,2], Zeshan Liang [1], Xiaobin Nan [3], Chunxu Jiang [1,*], Yong Li [1,2], Li Li [1], Liang He [2] and Shizheng Yang [2,*]

[1] Chongqing CEPREI Industrial Technology Research Institute Co., Ltd., Chongqing 401332, China; guoxiaotong0713@163.com (X.G.); liangzeshan@ceprei.com (Z.L.); 403ly@163.com (Y.L.); lili@ceprei.com (L.L.)
[2] China Electronic Product Reliability and Environmental Testing Research Institute, Guangzhou 511370, China; he_liang_mail@163.com
[3] College of Materials Science and Engineering, Taiyuan University of Technology, Taiyuan 030024, China; nanxiaobin0173@link.tyut.edu.cn
* Correspondence: jiangchunxu@ceprei.com (C.J.); yshzh1991@163.com (S.Y.); Tel.: +023-86968006 (C.J.); +020-32145846 (S.Y.)

Abstract: Turbine blades in aircraft engines may encounter overheating and suffer serious creep property degradation. In this study, the thermal cycling creep experiments were conducted on K465 superalloy under (900 °C/30 min–1100 °C/3 min)/50 MPa, (900 °C/30 min–1150 °C/3 min)/50 MPa and (1000 °C/30 min–1150 °C/3 min)/50 MPa. The investigated thermal cycling creep properties were dramatically degraded, and increasing the overheating temperatures significantly decreased the thermal cycling creep life. The secondary γ' precipitates obviously dissolved and the area fraction decreased to around 35.2% under (900 °C/30 min–1150 °C/3 min)/50 MPa and (1000 °C/30 min–1150 °C/3 min)/50 MPa, which was almost half that after the standard solution treatment. The decline of the thermal cycling creep properties was mainly due to the significant dissolution of γ' precipitates. The creep holes/cracks were mainly distributed at the M_6C carbides and γ/γ' eutectics interfaces, M_6C carbides and γ' film interfaces in the grain boundaries, and resulted in the final intergranular fracture.

Keywords: K465 alloy; overheating; creep; cracks

check for updates

Citation: Guo, X.; Liang, Z.; Nan, X.; Jiang, C.; Li, Y.; Li, L.; He, L.; Yang, S. Effect of Overheating Temperature on Thermal Cycling Creep Properties of K465 Superalloy. *Crystals* **2021**, *11*, 1458. https://doi.org/10.3390/cryst11121458

Academic Editors: Yanhui Chen, Yunsong Zhao and Bolv Xiao

Received: 5 November 2021
Accepted: 23 November 2021
Published: 25 November 2021

1. Introduction

Ni-based superalloys are generally selected as the materials of aircraft turbine blades [1,2]. During actual operation, the engine encounters emergencies such as inlet distortion [3] or one engine inoperative (OEI) conditions [4], which may result in a sharp temperature jump. This can pose a serious threat to the safe service of turbine blades, and the thermal cycling creep is always used to modify this specific service condition by airworthiness authorities such as European EASA [5].

Studies on thermal cycling creep have attracted attention since the 2010s due to the work of Cormier et al. on single-crystal Ni-based superalloys [5–9]. Recently, Guo et al. [10], Yuan et al. [11] and An et al. [12] began to investigate the thermal cycling creep behavior of equiaxed cast and directionally solidified superalloys, and Antonov et al. [13] briefly summarized the thermal cycling creep properties of conventionally cast, directionally solidified and single crystal superalloys. Overheating can result in the obvious dissolution of strengthening γ' precipitates, and thermal stress due to the temperature variation during the thermal cycling creep promotes the initiation of creep holes. The thermal cycling creep properties are even worse than those under overheating isothermal creep properties. However, there is still a lack of research on polycrystalline alloys, and the evolution law of thermal cycling creep properties of polycrystalline superalloys is not clear enough.

K465 superalloy is widely used to manufacture the aero-engine turbine blades, while the overheating service caused by the sudden temperature jump also poses a serious threat to its safe service [14]. Previous studies have shown that the thermal cycling creep property under (900 °C/30 min–1100 °C/3 min)/70 MPa was even worse when compared to the isothermal creep property under 1100 °C/70 MPa and 900 °C/70 MPa [10], while the effect of overheating temperature variation on the thermal cycling creep performance of the K465 alloy is still unclear. Exploring the above point is much more meaningful, considering that K465 alloy will encounter overheating at different temperatures, such as 1100 °C and 1150 °C.

In this study, we conducted three thermal cycling creep experiments on K465 superalloy to reveal the overheating effect on thermal cycling creep properties. The microstructure characterization and creep cracks were investigated. This study aims to briefly introduce the degradation law of the thermal cycling creep of conventionally cast superalloys.

2. Materials and Methods

All the as-received solid bars were manufactured using investment casting technology and experienced the standard solution treatment, which composed of solution treatment at 1210 °C for 4 h, followed by air cooling. The main chemical composition of K465 superalloy is Ni, 9.90 W, 9.50 Co, 8.66 Cr, 5.10 Al, 2.52 Ti, 1.44 Mo, 0.95 Nb, 0.16 C (in wt%). The microstructure morphologies have already been reported in Ref. [10]. The thermal cycling creep tests were conducted using our own creep testing rig, which has been systematically described in our previous article [10]. The normal allowable maximum service temperature of K465 alloy is 1000 °C and 1050 °C when used as turbine blades and vanes, respectively.

Figure 1a depicts the procedure of thermal cycling creep; creep temperature cycles were repeated at a temperature under 50 MPa. Each cycle consisted of a 30 min duration at lower temperature T_1, a 4 min heating from T_1 to T_2, a 3 min overheating at T_2 and a 5 min cooling from T_2 to T_1. Figure 1b depicts the size of the experimental specimen, and the gauge length and diameter was set as 40 mm and 5 mm, respectively. The creep tests under (900 °C/30 min–1100 °C/3 min)/50 MPa were interrupted after 191.8 h and the creep tests under (900 °C/30 min–1150 °C/3 min)/50 MPa and (1000 °C/30 min–1150 °C/3 min)/50 MPa were carried out until the samples fractured. It should be noted that the deformation is expressed by the total macro displacement of the sample. Table 1 shows the measured creep property with various overheating temperatures.

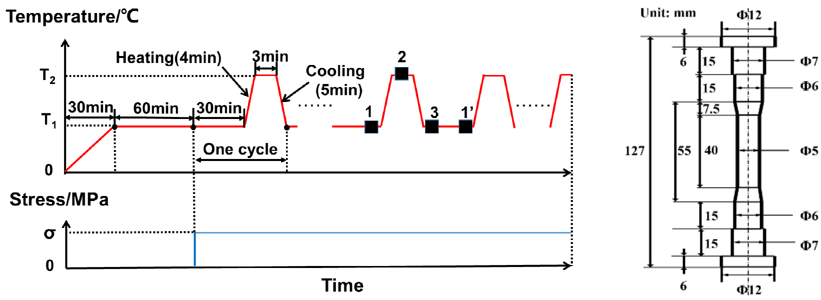

(**a**) (**b**)

Figure 1. (**a**) procedure of the thermal cycling creep testing. (**b**) size of the thermal cycling creep specimen.

Table 1. The creep testing conditions of the thermal cycling creep of K465 superalloy.

Specimen Number	T_1/°C	T_2/°C	Displacement/mm	Creep Time/h	Cycles
1#	900	1100	2.52	191.8	268
2#	900	1150	5.22	56.5	69
3#	1000	1150	6.47	20.4	26

Samples were prepared for microstructural observation after grinding and polishing. The detail etching method has been described in detail in Ref. [15]. Microstructural observations were conducted through a ZEISS AXIO image A2m optical microscope (OM) and ZEISS SUPRE 55 scanning electron microscope (SEM). The quantitative statistics of the area fractions of γ' precipitates were based on Chinese standard GB/T 15749-2008 through Photoshop software. At least three images were used to get a statistical result.

3. Results and Discussion

3.1. Thermal Cycling Creep Properties

Figure 2a presents the experimental creep deformation displacement vs. the time of the thermal cycling creep under (900 °C/30 min–1100 °C/3 min)/50 MPa (1# specimen). The overall displacement of the 1# specimen increased with extending the creep time, and the creep test was interrupted at the 269th cycle. A partially enlarged image of the creep curve is shown in Figure 2b. A displacement peak appears with the temperature jump, and is consistent with the reports by Cormier [16], Guo [10] and An [12] et al. Generally, the peak strain is caused by the changes in creep temperature, and consists of elastic strain, plastic strain and thermal strain. Figure 2c shows the experimental creep deformation vs. the time of the thermal cycling creep under (900 °C/30 min–1150 °C/3 min)/50 MPa (2# specimen) and (1000 °C/30 min–1150 °C/3 min)/50 MPa (3# specimen); the alloy fractured after 69 and 26 cycles, respectively. Under the above two conditions, the final fracture of the alloy occurred in the overheating stage of 1150 °C/3 min. After removing the elastic and thermal strains, the plastic strain was obtained [12]. Figure 2d depicts the plastic creep displacement vs. time curves under (900 °C/30 min–1100 °C/3 min)/50 MPa, (900 °C/30 min–1150 °C/3 min)/50 MPa and (1000 °C/30 min–1150 °C/3 min)/50 MPa. Obviously, increasing the creep temperatures T_1 and T_2 during the thermal cycle creep will significantly reduce the creep properties of the alloy.

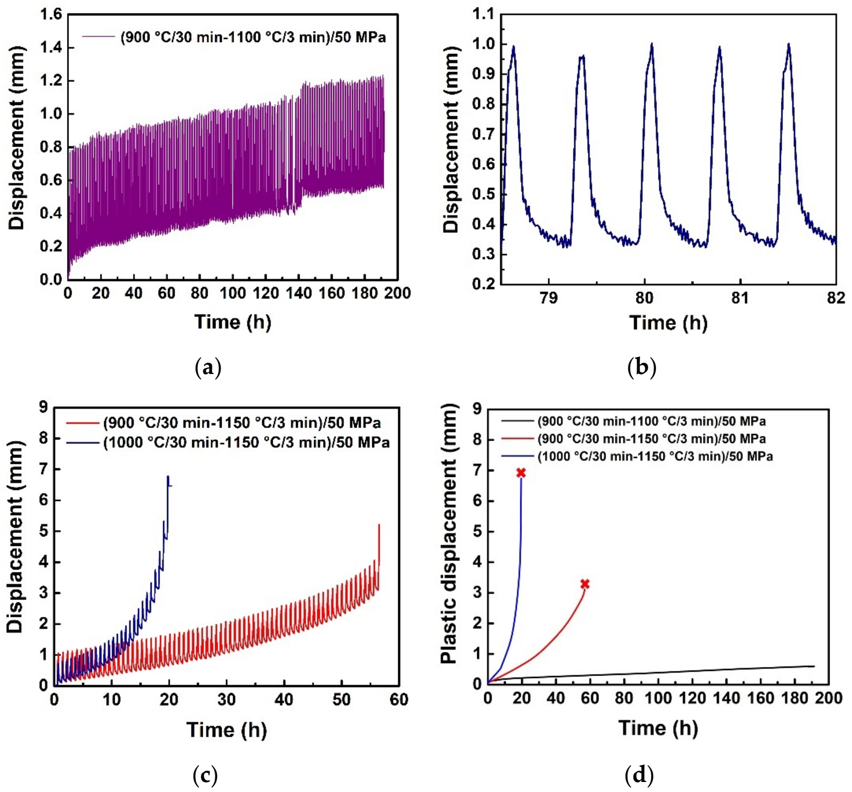

Figure 2. Experimental creep displacement vs. time of the thermal cycling creep under (900 °C/30 min–1100 °C/3 min)/50 MPa (**a**,**b**), (900 °C/30 min–1150 °C/3 min)/50 MPa and (1000 °C/30 min–1150 °C/3 min)/50 MPa (**c**). (**d**) plastic creep displacement vs. time curves under (900 °C/30 min–1100 °C/3 min)/50 MPa (interrupted), (900 °C/30 min–1150 °C/3 min)/50 MPa (fractured) and (1000 °C/30 min–1150 °C/3 min)/50 MPa (fractured).

3.2. Microstructure Characterizations

To reveal the overheating effect on the thermal cycling creep properties of K465 alloy, the main reinforcing phase γ' phase and creep voids were systematically characterized. The morphologies of the γ' precipitates in creep specimens 1# and 2# are shown in Figure 3a,b. For 1# specimen, the secondary γ' precipitates were obviously dissolved and directionally coarsened. It is worth noting that there were multiple ultra-fine γ' particles in the γ channel, and they were precipitated after the creep testing during the cooling process and are not concerned in the present work. When T_2 temperature rose to 1150 °C, the fracture microstructure showed that γ' precipitates dissolved more obviously, as shown in Figure 3b. The specific thermal exposure experiments of K465 alloy were carried out to analyze and evaluate the degradation of γ' phase. Figure 3c–e are SEM-SE images showing the morphologies of γ' precipitates in the dendrite core regions of K465 superalloy after being heat treated at 900 °C/1000 h 1100 °C/3 min and 1150 °C/3 min, respectively. The area fraction of γ' precipitates are listed in Table 2.

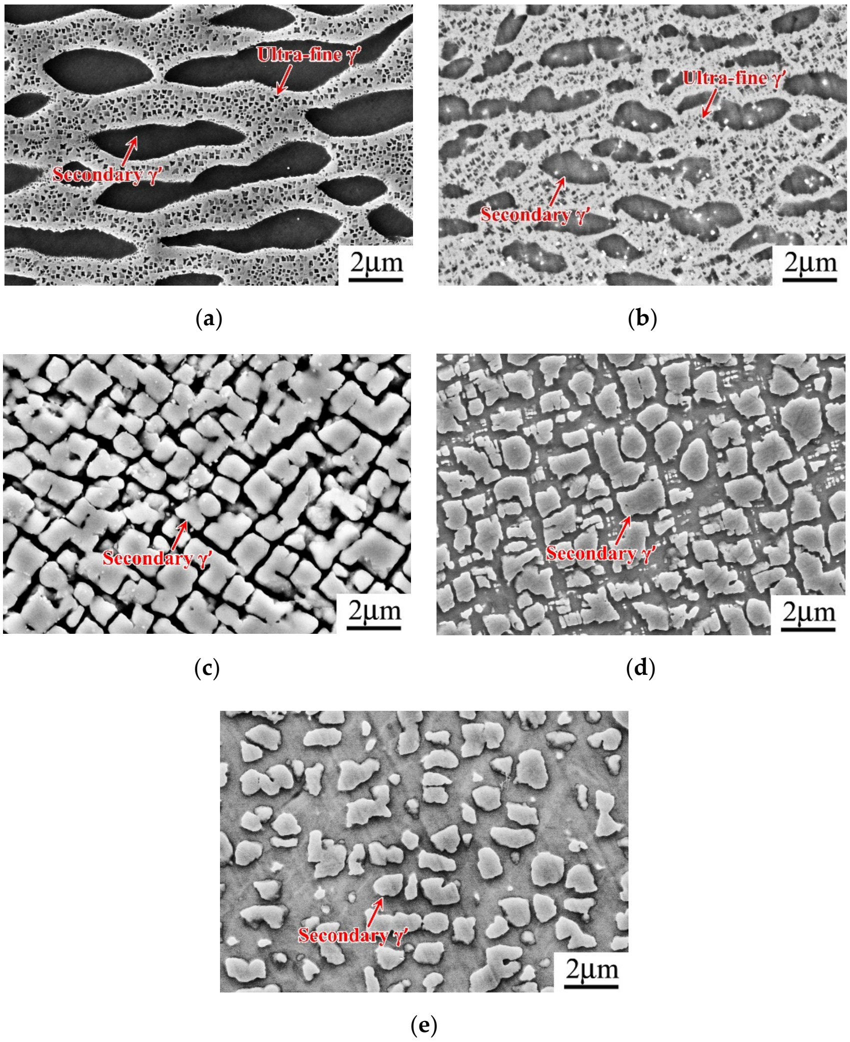

Figure 3. SEM-SE images of the γ' precipitates in the dendrite core regions at the longitudinal sections of creep specimens of K465 superalloy when creep under (900 °C/30 min–1100 °C/3 min)/50 MPa after 268 cycles (**a**) (900 °C/30 min–1150 °C/3 min)/50 MPa after 69 cycles (**b**) SEM-SE images of the γ' precipitates in the dendrite core regions of K465 superalloy after thermal exposure at 900 °C/1000 h (**c**) 1100 °C/3 min (**d**) and 1150 °C/3 min (**e**) followed by water cooling.

Table 2. Area fraction of γ' precipitates in the dendrite core regions of K465 superalloy after the standard solution treatment, during thermal cycling creep under different conditions and after heat treatment at 900–1150 °C.

Condition	Specimen Number	γ' Area Fraction/%	Interrupted Temperature/°C
Standard solution treatment	-	61.7 ± 1.4	-
Thermal cycling creep	1#	46.5 ± 3.2	1100
	2#	36.1 ± 1.8	1150
	3#	35.2 ± 2.4	1150
900 °C/1000 h	-	67.8 ± 1.2	900
1100 °C/3 min	-	50.5 ± 3.3	1100
1150 °C/3 min	-	34.1 ± 3.1	1150

In normal conditions (below 1000 °C), γ' precipitates basically maintained cubic morphology, as shown in Figure 3c. The area fraction of γ' phase kept 67.8 ± 1.2% after aging at 900 °C for 1000 h, even 6% larger than that after the standard solution treatment. This is mainly because the standard heat treatment temperature was semi solid solution treatment, and the forming elements of γ' phase are still supersaturated after air cooling. Therefore, when exposed to a relatively low heat treatment temperature of 900 °C, γ' phase precipitated completely, resulting in an increase of its area fraction [17]. The solvus temperature of γ' phase in the dendrite core region is 1210 °C [18]. After short-time overheating at 1100 °C and 1150 °C, significant dissolution of γ' phase occurred and the higher the temperature was, the more obvious this phenomenon was (Figure 3d,e). This is mainly due to the increase of the saturation of γ' phase enriched elements with the overheating temperature increasing, resulting in the decrease of area fraction of the γ' precipitates [18]. Especially after overheating treatment at 1150 °C, the area fraction of the γ' phase decreased to 34.1 ± 3.1%, which was only 1/2 of that after the standard heat treatment.

The temperature change will lead to the dissolution and re-reprecipitation of γ' precipitates continuously during the thermal cycling creep [10,12]. We previously identified that when crept under (900 °C/30 min–1100 °C/3 min)/70 MPa, γ' precipitates dissolved during the (T_1–T_2)/4 min and T_2/3 min stages, and partially recovered during the (T_2–T_1)/5 min and T_1/30 min stages [10]. The results of this study show that for the 1# specimen, the area fraction of the γ' precipitates decreased to 46.5 ± 3.2% and was even lower than that after overheating at 1100 °C/3 min, which may be due to the acceleration of stress on γ' dissolution during the creep process. For the 2# and 3# specimens, the area fractions of γ' precipitates were both close to that after overheating at 1150 °C/3 min, and the microstructural degradation of γ' precipitates was serious. However, it should be noted that the temperature T_1 of 2# specimen was 900 °C, which was lower than the 1000 °C of 3# specimen. Therefore, in other stages of the thermal cycling creep, including T_1/30 min stage, (T_1–T_2)/4 min stage, (T_2–T_1)/5 min stage, the area fraction of γ' precipitates in 2# specimen was higher than that in 3# specimen. More detailed characterizations of γ' phase microstructure are in progress, but it is certain that the significant γ' phase degradation is mainly responsible for the degradation of the thermal cycling creep of K465 superalloy. Whether T_1 or T_2, the higher the overheating temperature, the more serious the damage of thermal cycling creep performance (Table 1 and Figure 2).

At the same time, the weak regions in the process of thermal cycling creep, namely the creep hole/crack initiation regions, were systematically studied. Under the three creep conditions in this study, the distribution characteristics of creep holes/cracks were basically the same. Figure 4a,b are SEM-SE images showing the creep cracks distributed at the interfaces between M_6C carbides and γ/γ' eutectics when crept under (900 °C/30 min–1100 °C/3 min)/50 MPa and (900 °C/30 min–1150 °C/3 min)/50 MPa. Compared with the standard solution treated microstructure [19], the coupling effect of creep stress and cyclic thermal stress promoted the formation of M_6C carbides, resulting in the initiation of more creep holes/cracks. In addition, the interfaces of M_6C carbides and γ' film also easily initiated creep holes/cracks and lead to the final intergranular fracture (Figure 4c,d). Overall, the interfaces of M_6C carbides and γ/γ' eutectics in the interdendritic regions and that of M_6C carbides and γ' film in the grain boundaries easily initiated creep holes during the thermal cycling creep, and the creep cracks in the grain boundaries finally resulted in the intergranular fracture.

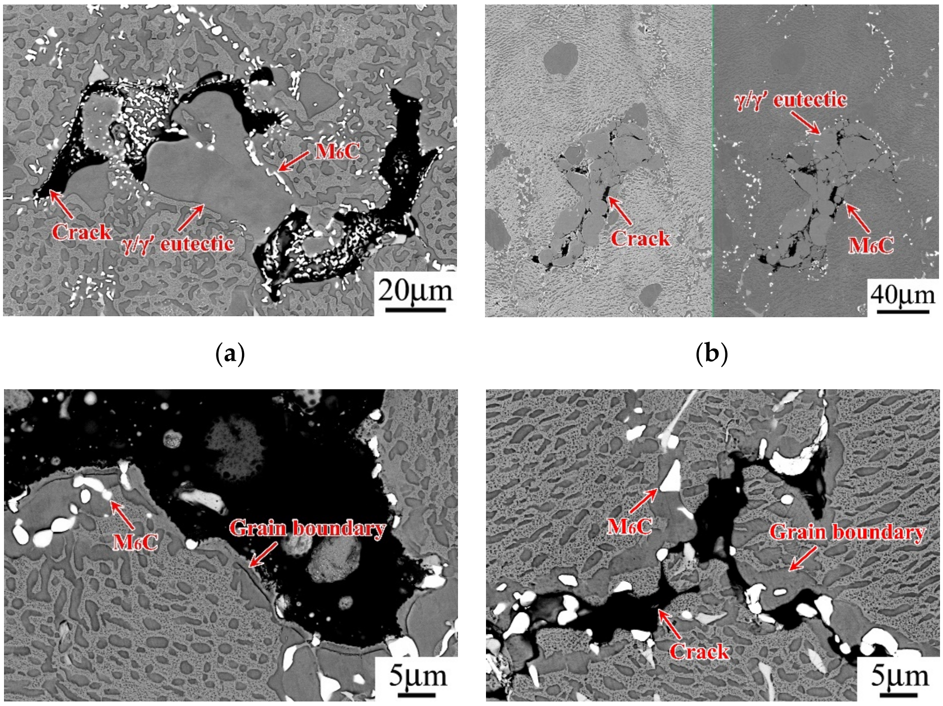

(**a**) (**b**) (**c**) (**d**)

Figure 4. SEM-BSE images of the creep cracks at the longitudinal sections close to the fracture surface of stress rupture specimens of K465 superalloy when creep under (900 °C/30 min–1100 °C/3 min)/ 50 MPa (**a**), (900 °C/30 min–1150 °C/3 min)/50 MPa (**b**,**c**), and (1000 °C/30 min–1150 °C/3 min)/ 50 MPa (**d**).

4. Conclusions

The thermal cycling creep was conducted under (900 °C/30 min–1100 °C/3 min)/ 50 MPa, (900 °C/30 min–1150 °C/3 min)/50 MPa and (1000 °C/30 min–1150 °C/3 min)/ 50 MPa. Combined with the systematic microstructural characterization, the overheating effect on thermal cycling creep properties of K465 superalloy was revealed. The main conclusions are summarized as follows:

(1) Creep life of thermal cycling creep was longer than 268 h under (900 °C/30 min–1100 °C/3 min)/50 MPa (268 cycles), while it decreased to 56.5 h and 20.4 h under (900 °C/30 min–1150 °C/3 min)/50 MPa (69 cycles) and (1000 °C/30 min–1150 °C/3 min)/50 MPa (26 cycles), respectively. Increasing the creep temperatures T_1 and T_2 may significantly decrease the thermal cycling creep property of K465 superalloy.

(2) The secondary γ' precipitates dissolved significantly, and the area fraction decreased to 46.5 ± 3.2%, 36.1 ± 1.8%, 35.2 ± 2.4% under (900 °C/30 min–1100 °C/3 min)/ 50 MPa, (900 °C/30 min–1150 °C/3 min)/50 MPa and (1000 °C/30 min–1150 °C/ 3 min)/50 MPa, respectively. The obvious degradation of γ' precipitates plays the most important role in the degradation of the thermal cycling creep properties.

(3) The creep holes/cracks were mainly distributed at the interfaces of M_6C carbides and γ/γ' eutectics, M_6C carbides and γ' film in the grain boundaries. Intergranular fracture finally occurred under the investigated thermal cycling creep conditions.

Author Contributions: Experiment conduction—X.G., Z.L.; data and image processing—Y.L., L.L., X.N.; writing—original draft preparation, X.G., L.H.; writing—review and editing, S.Y., C.J. All authors have read and agreed to the published version of the manuscript.

Funding: This research was funded by the Science and Technology Program of Guangzhou of China (Grant No. 202102020474), and CEPREI Innovation and Development Foundation (Grant No. 20Z33 and 20Z32).

Institutional Review Board Statement: Not applicable.

Informed Consent Statement: Not applicable.

Data Availability Statement: Not applicable.

Acknowledgments: The authors are grateful to Wenrui An from University of Science and Technology Beijing for his help on thermal cycling creep experiments.

Conflicts of Interest: The authors declare no conflict of interest.

References

1. Donachie, M.J.; Donachie, S.J. *Superalloys: A Technical Guide*; ASM International: Almere, The Netherlands, 2002; p. 8.
2. Reed, R.C. *The Superalloys: Fundamentals and Applications*; Cambridge University Press: New York, NY, USA, 2008; p. 372.
3. Tao, C.H.; Zhong, P.D. *Failure Analysis and Prevention for Rotor in Aero-Engine*; National Defense Industry Press: Beijing, China, 2008.
4. Le Graverend, J.B.; Cormier, J.; Caron, P.; Kruch, S.; Gallerneau, F.; Mendez, J. Numerical simulation of γ/γ' microstructural evolutions induced by TCP-phase in the MC_2 nickel base single crystal superalloy. *Mater. Sci. Eng. A* **2011**, *528*, 2620–2634. [CrossRef]
5. Cormier, J. Cycling creep resistance of Ni-based single crystal superalloys. In *Superalloys 2016: Proceedings of the 13th Intenational Symposium of Superalloys*; Wiley Online Library: Hoboken, NJ, USA, 2016; pp. 385–394.
6. Cormier, J.; Cailletaud, G. Constitutive modeling of the creep behavior of single crystal superalloys under non-isothermal conditions inducing phase transformations. *Mater. Sci. Eng. A* **2010**, *527*, 6300–6312. [CrossRef]
7. Cormier, J.; Milhet, X. Non-isothermal creep at very high temperature of the nickel-based single crystal superalloy MC_2. *Acta Mater.* **2007**, *55*, 6250–6259. [CrossRef]
8. Cormier, J.; Milhet, X. Non-isothermal creep behavior of a second generation Ni-based single crystal superalloy: Experimental characterization and modeling. In *Superalloys 2008: Proceedings of the 11th International Symposium of Superalloys*; Wiley Online Library: Hoboken, NJ, USA, 2008; pp. 941–949.
9. Le Graverend, J.-B.; Dirand, L. In Situ Measurement of the γ/γ' Lattice Mismatch Evolution of a Nickel-Based Single-Crystal Superalloy during Non-isothermal Very High-Temperature Creep Experiments. *Metall. Mater. Trans. A* **2012**, *43*, 3946–3951. [CrossRef]
10. Guo, X.; Zheng, W. High temperature creep behavior of a cast polycrystalline nickel-based superalloy K465 under thermal cycling conditions. *Materialia* **2020**, *12*, 100913. [CrossRef]
11. Yuan, X.; An, W. Evaluation of microstructural degradation and its corresponding creep property in integral cast turbine rotor made of K424 alloy. *Mater. Charact.* **2019**, *158*, 109946. [CrossRef]
12. An, W.; Utada, S. Thermal cycling creep properties of a directionally solidified superalloy DZ125. *J. Mater. Sci.* **2022**, *104*, 269–284. [CrossRef]
13. Antonov, S.; An, W. Evaluation and comparison of damage accumulation mechanisms during non-isothermal creep of cast Ni-based superalloy. In *Superalloys 2020: Proceedings of the 14th International Symposium of Superalloys Springer International, The Minerals, Metals & Materials Series*; Springer International Publishing: Cham, Switzerland, 2020; pp. 228–239.
14. Guo, X.; Zheng, W. Evaluation of microstructural degradation in a failed gas turbine blade due to overheating. *Eng. Fail. Anal.* **2019**, *108*, 308–317. [CrossRef]
15. Guo, X.; Antonov, S. Solidification rate driven microstructural stability and its effect on the creep property of a polycrystalline nickel-based superalloy K465. *Mater. Sci. Eng. A* **2020**, *770*, 138530. [CrossRef]
16. Cormier, J.; Jouiad, M. Very high temperature creep behavior of a single crystal Ni-based superalloy under complex thermal cycling conditions. *Philo. Mag. Lett.* **2010**, *90*, 611–620. [CrossRef]
17. Yuan, X.F.; Song, J.X. Quantitative microstructural evolution and corresponding stress rupture property of K465 superalloy. *Mater. Sci. Eng. A* **2016**, *651*, 734–744. [CrossRef]

18. Xiaotong, G.; Weiwei, Z. Microstructural degradation and tensile properties of K465 equiaxed-cast superalloy after short-time overheating. *J. Mater. Eng.* **2018**, *46*, 77–86.
19. Yuan, X.F.; Song, J.X. Abnormal stress rupture property in K465 superalloy caused by microstructural degradation at 975 °C/225 MPa. *J. Alloy Compd.* **2016**, *662*, 583–592. [CrossRef]